Dual-Rotor, Radial-Flux, Toroidally Wound, Permanent-Magnet Machines

Ronghai Qu, *Member, IEEE,* and Thomas A. Lipo, *Fellow, IEEE*

***Abstract*—A novel machine family—dual-rotor, radial-flux, toroidally wound, permanent-magnet (RFTPM) machines—is proposed in order to substantially improve machine torque density and efficiency. After the principles of operation, configurations, and features are discussed, the machine design and optimization guidelines are given. A prototype has been designed, built, and tested. The measured torque density of the prototype, which well matches the design value, is almost three times of that of the induction machine with the same power of 3 hp and speed. Meanwhile the efficiency is still kept high and the material cost is kept low by using ferrite magnets. Three novel approaches are proposed to reduce the cogging torque in the RFTPM machines, whose validity is verified by finite-element analysis results and experimental measurements.**

***Index Terms*—Cogging torque, electrical machine optimization, permanent-magnet (PM) machine design, radial-flux, toroidally wound, permanent-magnet (RFTPM) machines, toroidal windings.**

I. Introduction

HIGH torque density and high efficiency are two of the most desirable features for an electrical machine. Improvement of these features has been one of the main aspects of research on the electric machines in the last couple of decades. Several new topologies [1]–[7] have been proposed and improved torque density or efficiency was reported. Rare earth magnets, e.g., Neodymium–Iron–Boron (Nd–Fe–B), were used in these topologies to keep the efficiency high and achieve the high air-gap flux density and high torque density, which causes the material cost to be high. In addition, some topologies [6], [7] are restricted for low-speed applications since the losses quickly increase as the speed increases.

Development of a machine topology suitable for moderately high or high speed having high torque density and high efficiency simultaneously using such low-cost materials as ferrite magnets is challenging work and still continues to be a goal of electrical machine researchers. The purpose of this paper is to try to provide a solution to this problem by proposing and investigating a novel machine class—dual-rotor, radial-flux, toroidally wound, permanent-magnet (RFTPM) machines. Although a few radial-flux dual-rotor or dual-stator induction machines [8]–[11] and one dual-stator PM machines [3] have been reported, the dual-rotor, RFTPM machine topology is not well represented in the literature.

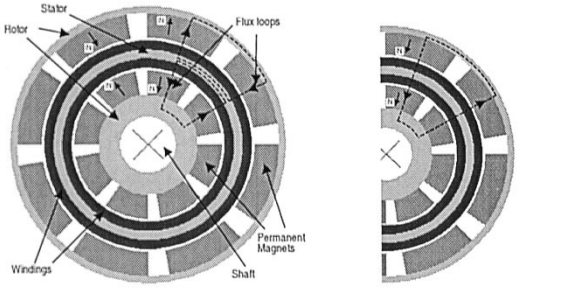

Fig. 1. Structure and flux distributions of dual-rotor, radial-flux, nonslotted, PM machine with surface-mounted magnets.

In this paper, the principles of operation, configurations, and features of the RFTPM machines are discussed. Three novel approaches to reduce cogging torque are proposed and verified by finite-element analysis (FEA) and experimental measurements to be valid. They are suitable for axial flux PM machines as well. In addition, machine design and optimization guidelines are discussed. A 3-hp dual-rotor RFTPM prototype machine that was designed, built, and tested is also reported. The experimental results of the prototype and comparison to conventional induction and interior PM machines are presented as well.

II. Structure and Principle of Operation

Briefly, the dual-rotor, RFTPM machine is constructed so that two machines are nested inside one another. The outer alternator has magnets at the outside surface of the outer air gap with the flux directed inward/outward, and the inner alternator has magnets at the inside surface of the inner air gap with the flux directed outward/inward, as shown in Fig. 1(a). The two sets of stator coils are back-to-back toroidally wound, sharing a common back iron. In this topology, the magnets drive flux across the two radial air gaps into the stator core; the flux then travels circumferentially along the core, back across the air gaps, and then through the rotor back iron.

The back electromotive force (EMF) is induced by the flux traveling circumferentially in the stator core. Since the directions of both current and flux for the inner air gap are opposite to that for the outer air gap, two tangential forces produced in

Paper IPCSD 03–085, presented at the 2002 Industry Applications Society Annual Meeting, Pittsburgh, PA, October 13–18, and approved for publication in the IEEE TRANSACTIONS ON INDUSTRY APPLICATIONS by the Electric Machines Committee of the IEEE Industry Applications Society. Manuscript submitted for review September 16, 2002 and released for publication July 18, 2003.

R. Qu is with Electronic and Photonic Systems Technologies, GE Global Research Center, Niskayuna, NY 12309 USA (e-mail: ronghaiqu@ieee.org).

T. A. Lipo is with the Department of Electrical and Computer Engineering, University of Wisconsin, Madison, WI 53706-1691 USA (e-mail: lipo@engr.wisc.edu).

Digital Object Identifier 10.1109/TIA.2003.818968

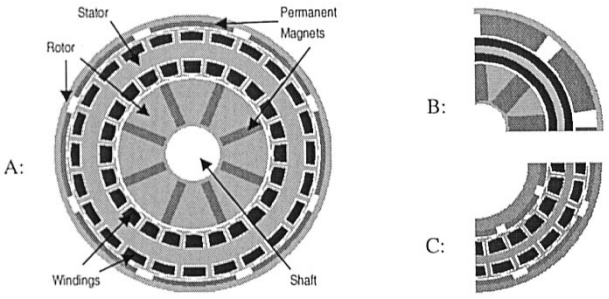

Fig. 2. Other dual-rotor RFTPM machine topologies. A: hybrid-PM with slots; B: hybrid-PM without slots; C: surface-PM with slots.

the inner and outer air gaps by interaction of the current commanded in the winding coils with the flux generated by the magnets have the same orientation. Since the working surfaces of the stator core are both used, in comparison with the conventional machines, the structure of this toroidal machine allows the exploitation of a higher percentage of the stator winding used for the production of machine torque.

In summary, the toroidal machine works like two conventional machines in series. One is inside, the other is outside. They have the same armature current. Their back EMFs are in series and may vary, depending on the air-gap flux densities. The outer and inner portion of the rotor are connected together by one end disc, which can work as a cooling fan. The stator is fixed at the other end to a frame.

III. Configurations and Features

A. Dual-Rotor Topologies

The dual-rotor, radial-flux machines can possess a variety of topologies based on different structure of windings, slots, and magnet arrangements. If back-to-back toroidal windings are used, the machines can be designated as RFTPM machines, as shown in Fig. 1(a), in which North–North (N–N) type magnet polarity arrangement is used. If both the inner and outer magnets are polarized in the same direction—North–South (N–S) type, the flux driven by the magnets will travel radially directly from inner rotor to outer or the reverse. For this case, as shown in Fig. 1(b), there is no flux traveling along the circumference of the stator core, so that no flux will link the back-to-back windings and the lap or wave windings should be used.

The stator core can also be slotted and the magnets can be not only surface mounted, but also buried, or a hybrid form with surface magnets for outer rotor and interior magnets for inner rotor. Fig. 2 shows three examples of the dual-rotor RFTPM machine structures with or without slots on the stator and with hybrid or surface magnets.

B. Torque Density and Efficiency

As a machine family, dual-rotor RFTPM machines have some specific features caused by their unique mechanical configuration: rotor–stator–rotor structure and double air gaps. Since the output torque is proportional to the air-gap surface area for the constant electrical and magnetic loadings, the first most straight forward observation coming from the doubled air gaps in a slightly enlarged volume is that the torque density will be substantially boosted. For the same machine outside diameter, the diameter of the outside air gap in the dual-rotor structure is larger than that in a conventional PM machine since the stator radial width including tooth and stator core is usually larger than the sum of the magnet thickness and the rotor core width. This situation implies that, for the same surface force density caused by the same surface current and airgap flux density, the torque produced in the outer air gap of the RFTPM structure is larger than that of the conventional PM machine. This is the second reason for the RFTPM machines to achieve a high torque density.

For the topologies with toroidally wound windings, the two working surfaces of the stator core are both used and the winding end portion is greatly shortened, which allows the machine to exploit a much higher percentage of the stator winding for the production of the machine torque in comparison to conventional machines. This results in an improved machine efficiency.

C. End-Winding Effects

The end-winding length in the RFTPM machines is not directly a function of the machine diameter and almost constant as the machine diameter increases. Consequently, the machine torque could be further improved by optimizing the machine aspect ratio of length to diameter. For two conventional induction or PM machines, M1 and M2, suppose that they have the same current density, flux densities, winding turns and distribution, speed, and machine overall, copper, and iron volumes, but M1 is longer and thinner than M2. It was found by using the scaling law that, if the end winding effect is not considered, M2 will achieve higher torque density than M1 [12]. Although the electrical loading of M2 is larger than M1, the copper loss in M2 is same as that in M1 due to the same current density and copper volume. In addition, more efficient cooling can be provided for M2 due to its larger diameter [13].

The reason conventional machines are not designed to have a shape of pancake by simply using this law is due to the long end winding, which almost linearly increases as the machine diameter increases. For conventional induction machines, the optimized aspect ratio varies depending pole numbers [14]. For the dual-rotor RFTPM machines, however, this law can be used since the end portion of the back-to-back winding is very short and keeps constant when the diameter increases. It is only a function of the air-gap flux density and pole number, not a function of the machine diameter. The total length of each coil is independent of the machine diameter, so do the winding resistance and the end winding leakage inductance. Although the second-order effects are neglected in the discussion above, it clearly demonstrates the desired ability of the dual-rotor RFTPM machines to improve torque and power densities by optimizing the aspect ratio. In addition, the ratio of the torque density of the dual-rotor RFTPM to conventional induction or PM machines increases as the rated power increases.

D. Magnets Materials and Limitations on Stator York Width

For the normal surface-mounted PM machines, rare-earth magnets, e.g., Nd–Fe–B, are necessary to provide the necessary flux density in the large air gap and thereby improve the relatively low torque density achieved by using ferrite magnets.

This requirement, however, is a common objection against PM machines since the use of Nd–Fe–B raises the cost of the machines. In dual-rotor, radial-flux machines, the substantially boosted torque density allows the use of the ferrite magnet. The material cost can therefore be sharply reduced.

For the structure with conventional windings, the stator core is unnecessary from the electromagnetic point of view due to the fact that no flux flows circumferentially, which is shown in Fig. 1(b). However, the stator core has to be retained for mechanical reasons, e.g., mechanically fixing the stator windings. The further investigation discloses that, even for those topologies with toroidal windings, if ferrite magnets are used, the limitation to reduce the stator core width is not the flux density in the stator core, but for mechanical reasons [12]. If rare-earth magnets are used, the situation may vary, depending on specific designs. This means that employing conventional windings can not necessarily reduce the stator yoke if ferrite magnets are used. In addition, the end winding is definitely much larger. Consequently, the efficiency could be similar to conventional PM machines and the torque density will not be as high as that in the topologies with toroidal windings.

E. Effects of Slotting and Surface or Interior Magnets

Smooth torque and low noise are advantages of the nonslotted configurations. Absence of slots and teeth implies a large air gap for the magnetic field associated with the currents in the windings. This suggests that the armature reaction is absent, which results in high overload capability, and that the back EMF in the stator windings does not change when the mechanical load of the machine varies. On the other hand, a large air gap requires using rare-earth magnets, which are currently still rather expensive. In addition, the low inductance can require high inverter switching frequency, raising the inverter losses.

In contrast, ferrite magnets can still achieve relatively high torque density in the slotted structure, which decreases the material cost and iron losses since less iron is required for ferrites due to the low magnet residual flux density. The cogging torque and associated noise can be reduced to a small level at minimal incremental cost by using three novel techniques, which will be proposed in Section IV.

The advantages of small armature reaction and high overload capability can also be achieved by selecting surface-mounted PMs. A large air gap, the main nature of both nonslotted and surface-mounted PM structures, in turn allows the rotor flux to remain unaffected by the currents in the stator. The uniform air gap provides a small and constant stator inductance which has traditionally been desirable in designing high response torque controllers albeit at the cost of elevated inverter switching losses.

It is well known that for surface-mounted PM machines there is no saliency effect, but for buried PM machines the properties are similar with those of salient-pole synchronous machines. For the dual-rotor hybrid PM machines (surface-mounted PM in outer rotor surface and buried in inner rotor), the difference between the d-axis reactance and q-axis reactance still exists but is relatively small.

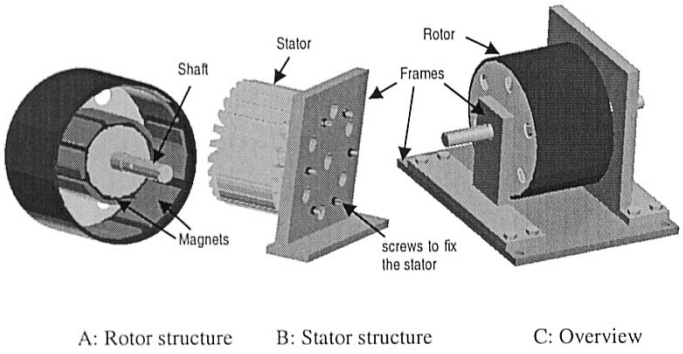

Fig. 3. Mechanical struture.

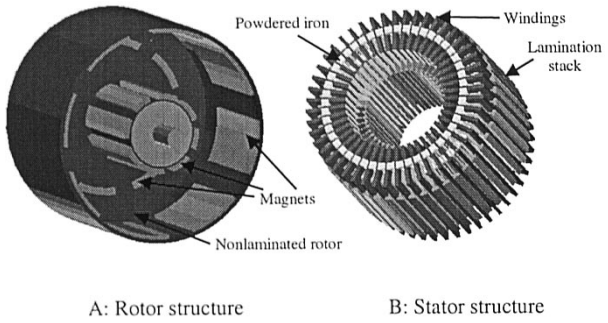

Fig. 4. Structure of an enhanced dual-rotor, slotted, RFTPM machine.

F. Radial Forces and Mechanical Structure

Another aspect for the dual-rotor topologies is that the radial forces, in addition to the alignment forces, are balanced. Radial forces are generated that attempt to close the air gap and bring the rotor and stator into contact with each other. In the topologies proposed, these forces are balanced by an equal and opposite attractive forces due to symmetry. In this case, the mechanical stress is ideally zero but in reality is nonzero but greatly reduced.

Fig. 3 demonstrates the mechanical structure which can be used for the RFTPM machine. The stator is fixed at one end to a frame. Two rotors are connected together by an end disc, which can be designed as a cooling fan to provide necessary cooling wind. Between the shaft and two frames there is one bearing set at each end. The cantilevered mechanical structure of the outside rotor and stator is a disadvantage, particularly as the speed increases. For large-power-level machines, the noncantilever structure, four bearings for this case, may be preferred. Since there are two air gaps to maintain, the relatively small mechanical tolerance or large air gaps are required. This is the other disadvantage of this topology.

G. Other Topologies

In order to further improve the machine efficiency, an enhanced dual-rotor topology may be used. Fig. 4(a) and (b) demonstrates the basic scheme of an enhanced dual-rotor, slotted, surface-mounted PM machine. From these sketches, note that, by mounting magnets on the surface of one of the two rotor ends in addition, the copper utilization percent is

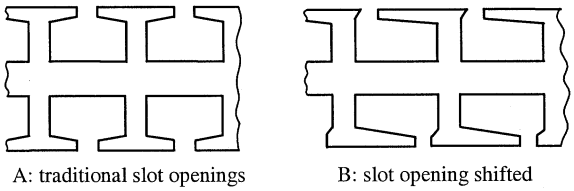

Fig. 5. Linear translational stator laminations with the different slot opening designs.

enhanced as well as the efficiency. However the question as to whether the overall torque density can be improved still depends on the stator yoke width and on the flux density in the end air gap.

Similar to the dual-rotor structure, the dual-stator topologies also can improve the torque density and efficiency by doubling the air gap and keeping the machine volume unchanged. Slotted or nonslotted structures, rare earth or ferrite magnets, and N–N-type or N–S-type magnets all can be used. The end winding in the dual-stator structure will be much longer than that in the dual-rotor structure since the nonback-to-back winding has to be used. This is a feature, however, that causes the efficiency and torque density to be lower.

IV. Cogging Torque

One of the disadvantages for surface PM machines is their cogging torque. Several techniques [15], [16] have been developed to reduce the cogging torque. These methods are also suitable for the dual-rotor RFTPM machines. In addition, the unique RFTPM machine structure of dual rotor and dual air gaps implies that there could be special techniques suitable for the dual-rotor RFTPM configuration. Given that the overall cogging torque of a RFTPM machine consists of the inner portion produced in the inner air gap and the outer portion produced in the outer air gap, the overall cogging torque can be reduced by two general approaches: reducing the amplitude of either or both of the inner and outer components, similar to what conventional methods accomplish, and shifting the relative phase of the two components so that they can compensate each other. Consequently, the overall cogging torque will be much reduced at minimal incremental cost. This approach does not distort the back-EMF waveform, and not reduce the average torque, nor enlarge the effective air gap.

In this paper, three specific approaches are presented. They are named as Varying Slot Opening Angular Width, Varying PM Angular Width, and Slot Opening Shifting.

A. Slot Opening Shifting

The idea of this approach is similar to the use of dummy slots but without any additional cost. The dual-rotor machines are easily designed to have a stator lamination with the inner and outer slot opening aligned in the radius direction as shown in Fig. 5(a). For this type slot design, the cogging torques produced by both the inner and outer air gaps are exactly in phase as shown by the dotted and dashed–dotted line in Fig. 6 (FEA results). Therefore, the amplitude of the total cogging torque will be their sum and larger than each components.

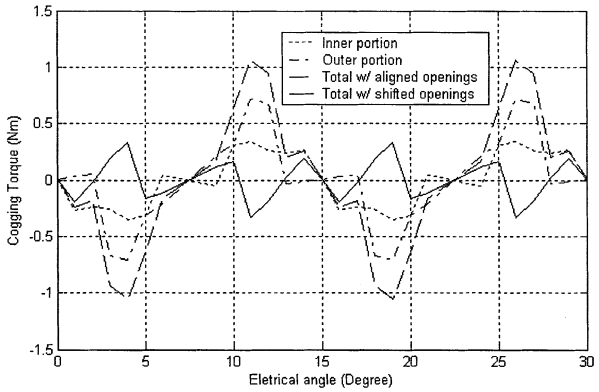

Fig. 6. Cogging torques achieved by different-type slot openings.

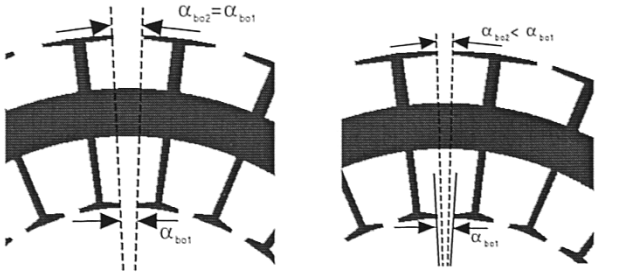

A: Same angular width: $\alpha_{bo1} = \alpha_{bo2}$ B: Different angular width: $\alpha_{bo1} > \alpha_{bo2}$

Fig. 7. Different designs of the slot opening angular widths.

If the slot openings in the inner and outer air gaps are shifted away by half of the slot pitch, as shown in Fig. 5(b), their cogging torque waveforms also will be phase shifted by 180°, so that the resultant total cogging torque is doubled in frequency and much reduced in amplitude. For this example, the amplitude of the cogging torque is reduced to less than one-third of the original by shifting the slot openings. This suggests that the proposed slot opening shifting is a valid approach to reduce the RFTPM machine cogging torque.

Since the inner and outer cogging torques have different amplitudes and waveforms, they cannot be exactly cancelled, even when they are 180° out of phase. However, by carefully designing the air gaps, magnet thickness, and length, similar amplitudes and waveforms can be achieved for the inner and outer cogging torques so that the overall cogging torque can be further reduced. It is interesting to note, for the same inner and outer magnet thickness, the larger the motor radius, the closer the amplitudes of the inner and outer portions of cogging torque are to each other. The slightly higher flux density in the inner air gap than in the outer air gap can achieve equal torque amplitudes.

B. Varying Slot Opening Angular Width

The slot openings at both sides of the stator can also be simply designed to have the same angular width, as shown in Fig. 7(a), in which there is no slot opening shifting. For this type of slot opening design, the cogging torques produced by both the inner and outer air gaps are exactly in phase. Consequently, the total

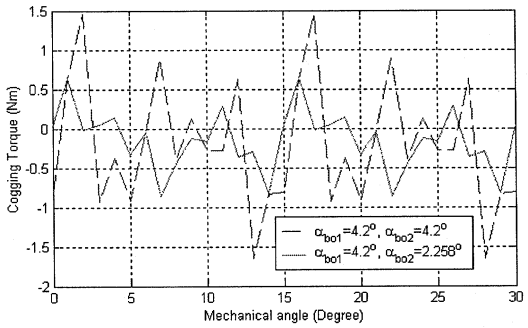

Fig. 8. Comparison of the cogging torques for the different slot-opening angular widths ($\alpha_1 = \alpha_2 = 40°$).

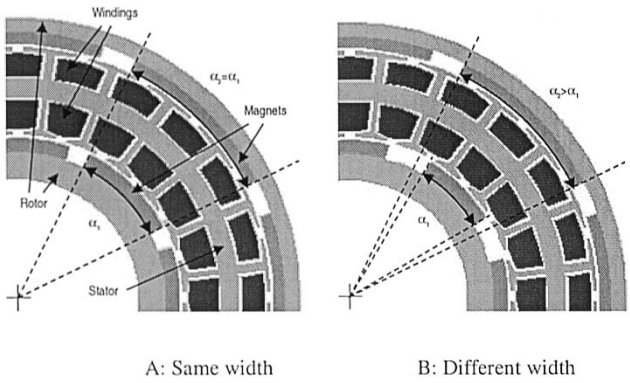

Fig. 9. Varying PM angular width for the inner and outer magnets.

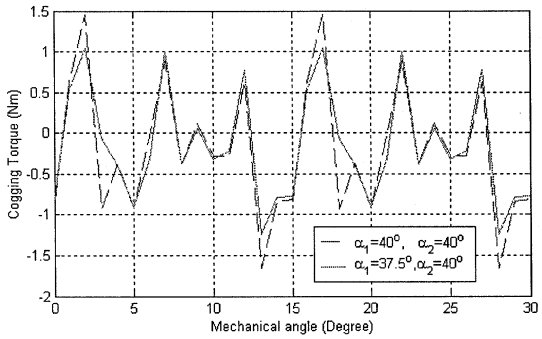

Fig. 10. Comparison of the cogging torques for the different PM angular widths ($\alpha_{bo1} = \alpha_{bo2} = 4.2°$).

cogging torque consisting in the inner and outer portions will be larger than each portion.

To reduce the total cogging torque, the outside slot angular width α_{bo2} can be designed to be smaller than the inside one α_{bo1}, since the outside slot opening arc is larger than the inside one for the same angular widths. A design example with the different angular widths for the slot openings is shown in Fig. 7(b). The waveform of the cogging torque produced by the inner air gap will be different as that by the outer air gap. Therefore, the overall cogging torque will be reduced.

Fig. 8 shows the FEA results of the examples shown in Fig. 7(a) and (b). The figure illustrates that the maximum value of the cogging torque is reduced by 50% to 0.8 N·m (the solid line) from the original 1.6 N·m (the dashed line) by changing α_{bo2} to 2.258° from 4.2°. This implies that the proposed varying slot opening approach is a valid approach to reduce the RFTPM machine cogging torque.

To reduce the cogging torque as much as possible, the two angles, α_{bo1} and α_{bo2}, must be carefully selected. Similarly to the slot opening shifting approach, this method cannot completely remove the cogging torque since the inner and outer cogging torques have the different amplitudes and waveforms. In addition, one needs to pay attention to the zigzag leakage flux, since it will be affected by the slot angular width.

C. Varying PM Angular Width

The two approaches discussed previously have achieved the same objective—reducing the overall cogging torque—by shifting away the maximum values of the inner and outer cogging torque. This objective can also be accomplished by varying the PM angular widths of the inner and outer magnets. The idea is depicted in Fig. 9. Fig. 9(a) shows a design with the same PM angular widths for the inner and outer magnets, whereas Fig. 9(b) shows the one with the different angular widths.

The cogging torque waveforms related to these designs are demonstrated in Fig. 10 by the dashed and solid lines, respectively. The maximum value of the cogging torque is reduced by designing the different PM angular widths for the inner and outer magnets, as expected. The peak value is reduced by almost 30% for this example, although the torque waveform dominated by the unchanged outer portion of the cogging torque is not greatly changed. Varying the magnet angular width affects the air-gap flux and leakage flux, which should also be considered in the design process.

All or two out of the three approaches discussed in this section can be employed together by carefully selecting each parameter mentioned in each approach to achieve the smallest cogging torque. The optimization process will be more complicated due to the coupling between any two of the three approaches. They also can be combined with any conventional techniques, e.g., skewing, to achieve even smaller cogging torque.

In addition, the proposed three techniques can be adopted in axial-flux PM machines with dual rotor or dual stator.

V. Design and Optimization Guidelines

Based on information in Sections II and III, the dual-rotor, toroidally wound surface PM topology with ferrite magnets and slots on the stator will be investigated further in Sections VI and VII and referred to simply as RFTPM machines. The toroidally wound windings can achieve higher torque density and efficiency than the conventional winding configurations. Ferrite magnets can keep the material cost and iron losses low, while slotting can keep the effective air gap in the reasonable range and the output torque density high. The cogging torque caused by slotting can be reduced by the proposed techniques so that the output torque ripple will be small.

The design process of the RFTPM machines is considerably more complicated than conventional surface PM machines due to the dual-rotor dual-air-gap structure and flux coupling in the stator yoke between the inner and outer portions. One may design either of two portions first, then design the other and check

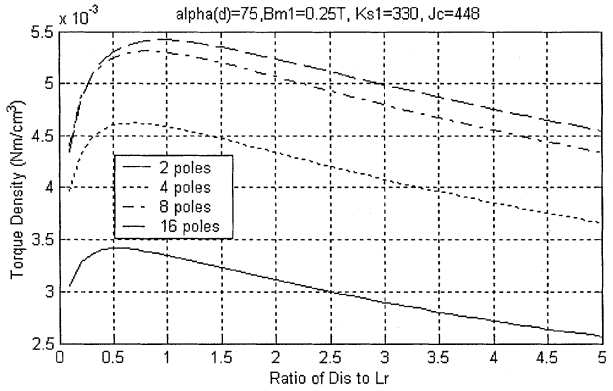

Fig. 11. Effect of the ratio of stator inner diameter $D_{\rm is}$ to machine effective length L_r on torque density.

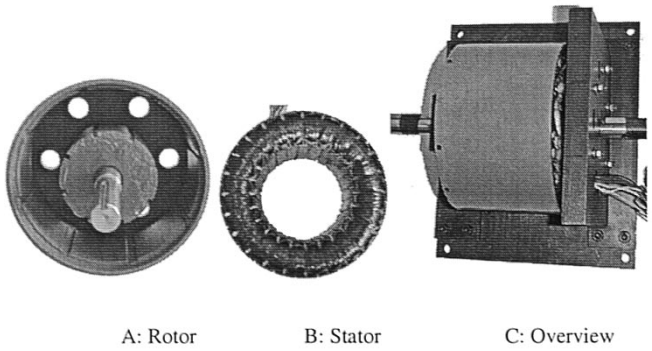

Fig. 12. Prototype machine.

if the stator yoke flux density is in the good range. Each portion of the design can be similar to the conventional surface PM design process, but the winding area, coil turns, and current density have to be the same for the two portions. To design a RFTPM machine with given power output, speed, efficiency, flux densities in the air gaps, and both stator and rotor iron, there will be an iteration in each inner or outer portion design and one more iteration to check if the required output power can be delivered.

In terms of optimization, the RFTPM machine is complicated as well since there are more variables to be optimized in the RFTPM machines: two air-gap flux densities, and two electrical loadings which couple together. One must optimize them together to find an optimal value set. Another main parameter that should be well optimized is the main aspect ratio of machine length to diameter, which will have different optimal value compared to that of conventional PM machines as shown in Fig. 11.

Fig. 11 clearly demonstrates the effect of ratio of the stator inner diameter $D_{\rm is}$ to the rotor length L_r and of pole numbers on the output torque of a three-phase, 3-hp, dual-rotor, RFTPM motor with a speed of 1800 r/min. The torque density can also be enhanced by selecting a high pole number, accepting the penalty of high iron losses.

VI. Machine Prototype and Experimental Measurements

A. Prototype Machine

A three-phase 3-hp dual-rotor RFTPM prototype shown in Fig. 12 was designed and built using ferrite magnets. The prototype was optimized to achieve the maximum torque density with efficiency of 87%. To more accurately calculate the airgap and zigzag leakage fluxes and optimize the torque density, two analytical leakage flux models [19] are proposed and used. The design parameters for the prototype are as follows:

torque	12.87 N·m;
efficiency	87%;
dc-bus voltage	380 V;
speed	1800 r/min;
windings	24 slots, 46 turns/slot;
trapezoidal phase current	9.1A, peak

For good heat management, the end portion of the rotor should be design as a cooling fan. As the first prototype, a few holes were simply punched to provide some cooling for the stator.

A special type of winding machine is commercially available to wind the toroidal windings. For the prototype, the windings were wound by hand. An alternative winding approach is cutting the stator core into two or more pieces, winding each piece separately, then assembling the stator.

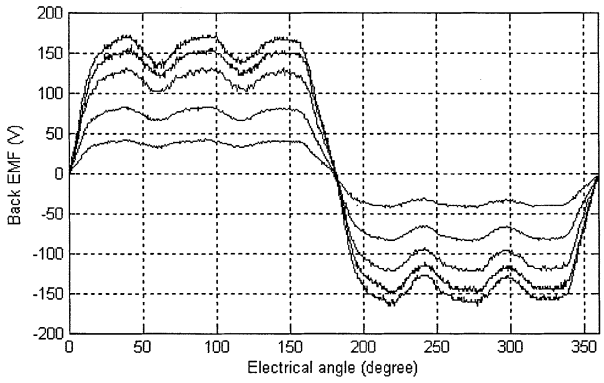

Fig. 13. Open-circuit back-EMF waveforms of Phase A at 500, 1000, 1500, 1800, and 2000 r/min.

TABLE I
VARIABLE-FREQUENCY PERFORMANCE

Speed	Output Torque	Output Power	Input Power	Efficiency	Power Factor
RPM	Nm	HP	HP	%	
500	12.35	0.87	1.17	74.2	0.68
1000	12.35	1.73	2.05	84.4	0.74
1500	12.28	2.59	2.94	88.0	0.76
1800	12.35	3.12	3.49	89.5	0.78

B. Back EMF, Variable Frequency, and Load Performance

The prototype was driven by the rectangular current using a digital-signal-processor (DSP)-based three-phase inverter. The open-circuit back EMF shown in Fig. 13 is linearly increases as the speed increase from 0 to 2000 r/min. The small ripples in the back-EMF waveforms are caused by slotting on the stator The variable frequency performance was tested first by injecting rated phase current, which was aligned with the phase back EMF to produce the maximum output torque. The experimental results illustrated in Table I show that the prototype can deliver constant output torque and power. The results are slightly higher than the design values at all the testing points. The efficiency and

TABLE II
VARIABLE-LOAD PERFORMANCE

Current	Output Torque	Output Power	Input Power	Efficiency	Power Factor
A, rms	Nm	HP	HP	%	
0.24	0	0	0.09	0	0.79
1.85	3.05	0.77	0.88	87.4	0.80
4.19	7.12	1.80	1.98	90.9	0.83
5.94	10.26	2.59	2.86	90.5	0.81
7.15	12.35	3.12	3.49	89.5	0.78

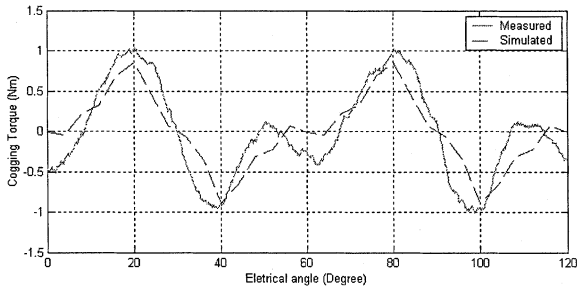

Fig. 14. Cogging torque of the prototype.

power factor are both in a reasonable range. The variable load testing summarized in Table II was then performed at the rated speed of 1800 r/min. As the phase current increases to the rated value of 7.15 A (rms) from 0, the output torque almost linearly increases (refer to Fig. 15), as expected. Both the highest efficiency of 90.9% and highest power factor of 0.83 were achieved at approximately 60% load.

Due to the small stator lamination volume and the low flux density in the stator yoke (0.8 T, required only by mechanical considerations), the iron losses are only 10% of the total losses at the rated operation point, while copper loss is more than 67%. Since copper loss compared to iron losses is relatively much easier to predict, the total losses can be predicted more accurately.

C. Cogging Torque

Two of three techniques proposed in Section IV—Varying Slot Opening Angular Width and Varying PM Angular Width—were employed to achieve the low cogging torque in the prototype. The FEA results (the dashed line in Fig. 14) matches well the measured cogging torque (the solid line in Fig. 14). The maximum cogging torque of 1 N·m is observed, which is 8.4% of the rated torque. Given that no common techniques, such as skewing, were utilized in this prototype, 8.4%, compared to the typical 20% [17] for the surface-mounted PM machines, can be considered as small. If the slot opening shifting is used, the cogging torque could have been reduced further.

D. Overload Capability and Temperature Effects

As a surface PM machine, the prototype is expected to have strong short-period overload capability. This is illustrated in Fig. 15, in which 126% of the rated output torque is observed when 130% phase currents are injected at the reduced speed of 1000 r/min. Due to the inverter current and voltage limitations, further high load operations are simulated by FEA only and the

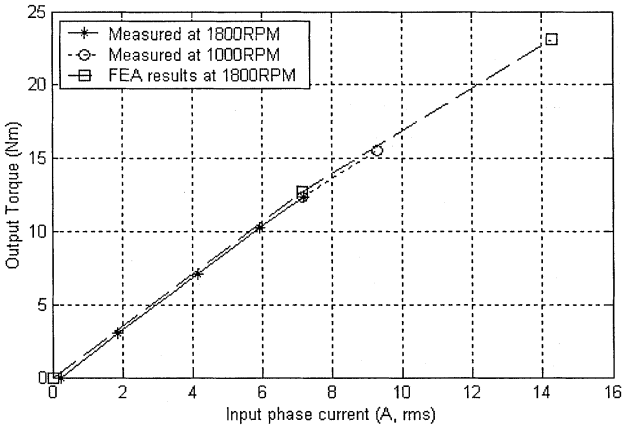

Fig. 15. Output torque versus input phase current.

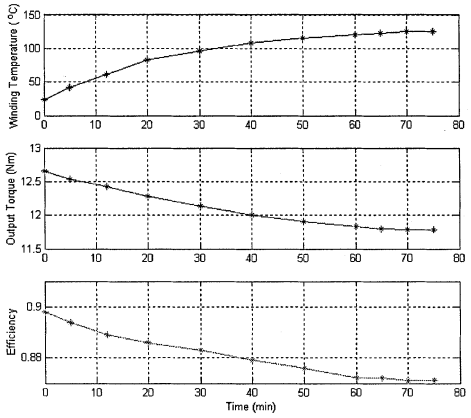

Fig. 16. Temperature effect on torque and efficiency.

results are depicted in Fig. 15 (dashed line), in which 182% of the rated torque is obtained when the 200% rated phase current are injected. The FEA results match well the experimental measurements and predicts the strong overload capability.

It is well known that, as the machine temperature increases, the copper resistance as well as the copper losses increases, while the magnet residual flux density and the output torque decrease. To prove whether the machine temperature is in the reasonable range and whether the prototype is able to deliver the continuous rated power at the rated speed, a temperature rise test at rated speed and rated load was carried out and shown in Fig. 16, in which the winding temperature was calculated by measuring the phase resistance [18]. The motor was driven at rated speed of 1800 r/min and rated phase current of 7.15 A (rms) and maintained during the test interval (the peak current was adjusted to keep the rms value unchanged). The phase-*A* voltage and current, phase-*B* current, and output torque waveforms at the steady state are recorded and shown in Fig. 17.

The winding temperature reached 125 °C in 70 min and remained stable at this temperature, while the resistance of phase *A* increased almost by 40% to 1.53 Ω from the original 1.1 Ω. Since the higher temperature causes the magnet residual flux density to decrease, the output torque decreased to 98.8% (2.98 hp) from 106.1% of the rated value. The input power also decreased due to the lower induced back EMF at the high temperature. The machine overall efficiency achieved at the steady-state

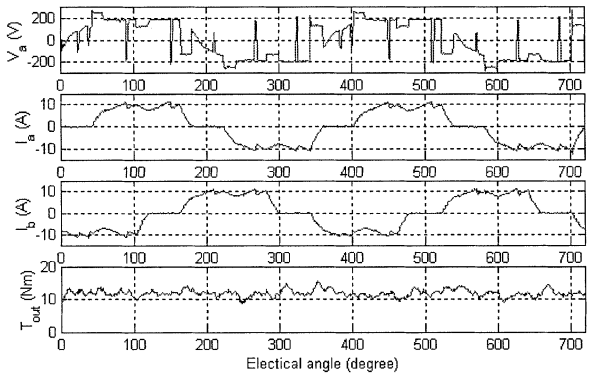

Fig. 17. Steady-state test waveforms at rated speed and rated load.

TABLE III
ACTIVE MATERIAL VOLUME, WEIGHT, AND COST

		Magnet	Copper	Iron	Total[b]
Prototype (Ferrite)	Volumn (cm^3)	195	772	705	2353
	Mass (kg)	1.0	3.4	5.4	9.8
	Cost (S)[a]	5.63	14.7	7.1	27.43
Alternative (NdFeB)	Volumn (cm^3)	40	451	587	1409
	Mass (kg)	0.3	2.0	4.5	6.8
	Cost (S)[a]	26.4	8.5	5.9	40.8

a: 5.5$/kg for ferrites; 77$/kg for NdFeb; 4.4.$/kg for copper; 1.32$/kg for laminations
b: volumn is the overall machine volumn, mass and cost are for active materials only.

winding temperature is 87.1%, which well matches the design efficiency 87%. In addition, the connection portion between inner and outer rotors can be well designed as a cooling fan to provide the even better cooling condition to further improve the current density and torque density.

E. Active Material Cost

Table III gives the active material volume, mass, and cost for the prototype. In addition, an equivalent alternative design using Nd–Fe–B magnets is provided for comparison purposes. Table III illustrates that the total active material cost of the alternative design is higher than that of the prototype by more than 30% due to the increased magnet cost, although the copper and iron costs are much lower in the alternative design.

VII. EVALUATION

The torque density, ratio of torque to weight, and efficiency of the prototype have been compared with a commercial induction motor (IM) and an interior PM (IPM) machine. All three machines are air cooled. Table IV shows that the proposed RFTPM motor has a much higher torque density and the ratio of torque to weight than the other two machines. Its torque density is almost three times that of the induction machine and 2.2 times the IPM machine's, while its efficiency is kept as high as 87%, which is only slightly lower than the IPM machine, but higher than the induction machine. Given that the IPM machine is 5 hp and was built using Nd–Fe–B magnets, and that both its torque density and efficiency should be considerably higher than a similar 3-hp machine, the efficiency of the RFTPM machine of the same 5-hp rating would almost certainly be greater. These data

TABLE IV
COMPARISON OF THE TORQUE DENSITY AND EFFICIENCY

Parameters	IM[a]	IPM[c] (NdFeB)	RFTPM (Ferrite)
Rated Power (HP)	3	4.96	2.98
Rated Torque (Nm)	12.18	20.2	11.78
Rated Speed (RPM)	1755	1750	1800
Machine Volume (cm^3)	8092[b]	10391	2730
Weight (kg)	35.4	48	11.76
Torque versus weight (Nm/kg)	**0.344**	**0.421**	**1.002**
Torque density (Nm/cm^3)	0.00151	0.00194	0.00432
Normalized Torque Density	**1**	**1.285**	**2.861**
Efficiency	0.825	0.88	0.871

a: GE motor with model # 5K182BC218A. c: Yaskawa Electric Co. motor
b: Excluding room for the fan and heat sink.

imply that the material cost will be much lower for the RFTPM machine than IM and IPM machines due to the relatively much smaller volume and use of ferrite magnets.

If a proper method is used to fix the inner magnets, or the hybrid magnet topology is used, the dual-rotor RFTPM machine could be operated at moderately high or high speed, due to its low iron and total losses.

VIII. CONCLUSION

A novel machine family—dual-rotor, RFTPM machines—was proposed in order to improve machine torque density and efficiency. Several topologies and their features are discussed, and machine design and optimization guidelines are given.

It has been proven that the dual-rotor, RFTPM machines can substantially improve the efficiency due to the greatly shortened end windings and sizably boost the torque density by doubling the working portion of the air gap as well as optimizing the machine aspect ratio. The ratio of the torque densities between the dual-rotor RFTPM and conventional induction machines increases as the power increases. The material cost is also kept low by using ferrite magnets.

The RFTPM machine was proven to be suitable for the moderately high speed and shows the potential for even higher speed. In addition, the cogging torque and associated noise can be reduced to a very low level at minimal additional cost or penalty by using the proposed three techniques, which can also be used for axial flux PM machines.

This machine could be a potential candidate in many cases, especially suitable for cases where an outside rotor is preferred, such as fans and electric automobile motors. In addition, it could be a good competitor with the strong potential in the aerospace industry due to its high torque density and high efficiency.

REFERENCES

[1] Y. Liao, F. Liang, and T. A. Lipo, "A novel permanent magnet motor with doubly salient structure," in *Conf. Rec. IEEE-IAS Annu. Meeting*, vol. 1, Houston, TX, 1992, pp. 308–316.
[2] X. Luo, D. Qin, and T. A. Lipo, "A novel two phase double salient permanent magnet motor," in *Conf. Rec. IEEE-IAS Annu. Meeting*, vol. 2, San Diego, CA, 1996, pp. 808–815.
[3] A. Toba and T. A. Lipo, "Novel dual-excitation permanent magnet vernier machine," in *Conf. Rec. IEEE-IAS Annu. Meeting*, vol. 4, Phonix, AZ, 1999, pp. 2539–2544.

[4] F. Profumo, A. Tenconi, Z. Zhang, and A. Cavagnino, "Novel axial flux interior PM synchronous motor realized with powdered soft magnetic materials," in *Conf. Rec. IEEE-IAS Annu. Meeting*, vol. 1, St. Louis, MO, 1998, pp. 152–158.
[5] F. Caricchi, F. Crescimbini, and O. Honorati, "Low-cost compact machine for adjustable—Speed pump application," *IEEE Trans. Ind. Applicat.*, vol. 34, pp. 109–116, Jan./Feb. 1998.
[6] J. Luo, S. Huang, S. Chen, and T. A. Lipo, "Design and experiments of a novel axial flux circumferential current permanent magnet (AFCC) machine with radial airgap," in *Conf. Rec. IEEE-IAS Annu. Meeting*, vol. 2, Chicago, IL, 2001, pp. 1989–1996.
[7] D. Qin, R. Qu, and T. A. Lipo, "A novel electric machine employing torque magnification and flux concentration effects," in *Conf. Rec. IEEE-IAS Annu. Meeting*, vol. 1, Phonix, AZ, 1999, pp. 132–139.
[8] M. M. E. Missiry, "Theory and performance of double-stator hollow rotor motor," in *Conf. Rec. IEEE-IAS Annu. Meeting*, vol. 1, Atlanta, GA, 1987, pp. 760–767.
[9] T. A. Lipo, "Analog computer simulation of an axially aligned two rotor A.C. machine," Master's thesis, Dept. Elect. Comput. Eng., Marquette Univ., Milwaukee, WI, 1964.
[10] D. H. Kelly, "Double-rotor induction motor," *IEEE Trans. Power App. Syst.*, vol. PAS-88, pp. 1086–1092, July 1969.
[11] C. W. Olliver, "Super-synchronous motors," *Power Engineer*, vol. 23, no. 268, pp. 269–271, July 1928.
[12] R. Qu, "Design and analysis of dual-rotor, radial-flux, toroidally-wound, surface-mounted-PM machines," Ph.D. dissertation, Dept. Elect. Comput. Eng., Univ. Wisconsin, Madison, WI, 2002.
[13] T. J. E. Miller, *Brushless Permanent-Magnet and Reluctance Motor Drives*. Oxford, U.K.: Clarendon, 1989.
[14] T. A. Lipo, *Introduction to AC Machine Design*. Madison, WI: Wisconsin Power Electronics Res. Center, Univ. of Wisconsin, 1998.
[15] T. M. Jahns and W. L. Soong, "Pulsating torque minimization technique for permanent magnet AC motor drives—A review," *IEEE Trans. Ind. Electron.*, vol. 43, pp. 321–330, Apr. 1996.
[16] N. Bianchi and S. Bolognani, "Design techniques for reducing the cogging torque in surface-mounted PM motors," in *Conf. Rec. IEEE-IAS Annu. Meeting*, vol. 1, Rome, Italy, 2000, pp. 179–185.
[17] T. Li and G. Slemon, "Reduction of cogging torque in permanent magnet motors," *IEEE Trans. Magn.*, vol. 24, pp. 2901–2903, Nov. 1988.
[18] S. Huang, *Electrical Machine Testing Technology* (in Chinese). Shanghai, China: Shanghai Univ. of Technology Press, 1990.
[19] R. Qu and T. A. Lipo, "Analysis and modeling of airgap and zigzag leakage fluxes in a surface-mounted-PM machine," in *Conf. Rec. IEEE-IAS Annu. Meeting*, vol. 4, Pittsburgh, PA, 2002, pp. 2507–2513.

Ronghai Qu (S'01–M'02) is a native of China. He received the B.E.E. and M.S.E.E. degrees from Tsinghua University, Beijing, China, in 1993 and 1996, respectively, and the Ph.D. degree in electrical engineering from the University of Wisconsin, Madison, in 2002.

From 1996 to 1998, he was a faculty member of the Electrical Engineering Department, Tsinghua University, and in 1998, he joined the Wisconsin Electric Machines and Power Electronics Consortium (WEMPEC) as a Research Assistant. He became a Senior Electrical Engineer at Northland, a Scott Fetzer Company, in 2002, and in 2003, he joined the GE Global Research Center, Niskayuna, NY, where he is presently an Electrical Engineer in the Electric Machines and Drives Laboratory. He has authored 13 published technical papers and has two U.S. patents pending and several disclosures.

Dr. Qu received the President Jiang Nanxiang Award from Tsinghua University in 1992. He received the Third Prize Paper Award from the Electric Machines Committee of the IEEE Industry Applications Society (IAS) for presentations at the 2002 IAS Annual Meeting.

Thomas A. Lipo (M'64-SM'71-F'87) was born in Milwaukee, WI. He received the B.E.E. and M.S.E.E. degrees from Marquette University, Milwaukee, WI, in 1962 and 1964, respectively, and the Ph.D. degree in electrical engineering from the University of Wisconsin, Madison, in 1968.

From 1969 to 1979, he was an Electrical Engineer in the Power Electronics Laboratory of Cooperate Research and Development of the General Electric Company, Schenectady, NY. He became a Professor of Electrical Engineering at Purdue University, West Lafayette, IN, in 1979, and in 1981, he joined the University of Wisconsin, Madison, in the same capacity, where he is presently the W. W. Grainger Professor for Power Electronics and Electrical Machines, Co-Director of the Wisconsin Electric Machines and Power Electronics Consortium, and Director of the Wisconsin Power Electronics Research Center. He has authored 400+ published technical papers and is the holder of 32 U.S. patents.

Dr. Lipo has received the 1986 Outstanding Achievement Award from the IEEE Industry Applications Society (IAS), William E. Newell Award of the IEEE Power Electronics Society, and the 1995 Nicola Tesla IEEE Field Award from the IEEE Power Engineering Society for his work. He has served the IEEE in various capacities for three IEEE Societies, including President of the IAS. He is a Fellow of the Institution of Electrical Engineers, U.K., and the Royal Academy of Engineering (Great Britain), and a Member of the Institute of Electrical Engineers of Japan. He has received 21 IEEE Prize Paper Awards from three different IEEE Societies including Best Paper Awards for publication in the IEEE TRANSACTIONS in the years 1984, 1994, and 1999.